Journal of Hazardous Materials 193 (2011) 296–303

Contents lists available at ScienceDirect

Journal of Hazardous Materials

journal homepage: www.elsevier.com/locate/jhazmat

Removal of arsenic and methylene blue from water by granular activated carbon media impregnated with zirconium dioxide nanoparticles

Robert Sandoval, Anne Marie Cooper, Kathryn Aymar, Arti Jain, Kiril Hristovski*

Environmental Technology, College of Technology and Innovation, Arizona State University, 6073 S. Backus Mall, Mesa, AZ 85212, United States

ARTICLE INFO

Article history:
Received 22 March 2011
Received in revised form 27 June 2011
Accepted 16 July 2011
Available online 7 August 2011

Keywords:
Nanoparticle
Zirconium dioxide
Arsenic
Methylene blue
Granular activated carbon

ABSTRACT

This study investigated the effects of in situ ZrO_2 nanoparticle formation on properties of granulated activated carbon (GAC) and their impacts on arsenic and organic co-contaminant removal. Bituminous and lignite based zirconium dioxide impregnated GAC (Zr–GAC) media were fabricated by hydrolysis of zirconium salt followed by annealing of the product at 400 °C in an inert environment. Media characterization suggested that GAC type does not affect the crystalline structure of the resulting ZrO_2 nanoparticles, but does affect zirconium content of the media, nanoparticle morphology, nanoparticle distribution, and surface area of Zr–GAC. The arsenic removal performance of both media was compared using 5 mM $NaHCO_3$ buffered ultrapure water and model groundwater containing competing ions, both with an initial arsenic $C_0 \approx 120$ μg/L. Experimental outcomes suggested favorable adsorption energies and higher or similar adsorption capacities than commercially available or experimental adsorbents when compared on the basis of metal content. Short bed adsorber column tests showed that arsenic adsorption capacity decreases as a result of kinetics of competing ions. Correlation between the properties of the media and arsenic and methylene blue removal suggested that surface area and GAC type may be the dominant factors controlling the arsenic and organic co-contaminant removal performance of the fabricated Zr–GAC media.

1. Introduction

Many water sources in small and rural communities are contaminated with multiple contaminants, some of which have completely different chemistries that require complex treatment trains for adequate removal from water. However, such technologies cannot be implemented in small and poor rural communities because of absence of technical knowledge among the residents and unsustainable costs of construction, operation and management of multiple treatment train units. Nevertheless, a need for providing potable water for residents of these communities via simple and inexpensive water treatment systems still exists.

Arsenic is one of the most common water contaminants that can be found in drinking water sources of many small and rural communities throughout the world with concentrations often exceeding 500 μg/L [1–3]. The maximum mandated, or recommended, contaminant levels for arsenic, however, can be as much as 10–50 times lower depending on a country's regulations [4–6]. Recent risk assessment studies suggest that allowable levels of arsenic in water should be lowered further to 0.1 μg/L because of arsenic's toxicity and carcinogenicity [7,8]. Arsenic has a unique chemistry which allows it to exist as an oxo-anion in natural waters regardless of whether it exists in arsenite (+3) or arsenate (+5) form, the two most dominant forms of arsenic in water [9–11]. The oxo-anion configuration allows arsenic to interact with metal (hydr)oxide surfaces by forming monodentate and bidentate inner-sphere complexes [12]. This interaction makes many of the metal (hydr)oxide materials suitable media for removal of arsenic from water by adsorption [13].

Many water sources in small and rural communities contain natural organic matter or organic contaminants in higher concentrations than arsenic as a result of natural or anthropogenic impacts. In many cases, these organic contaminants can be removed from water by adsorption using granulated activated carbon (GAC) [14]. Unlike metal (hydr)oxides, granulated activated carbon has been proven to be a poor adsorbent for treating arsenic [15]. However, recent studies have shown that arsenic and organic co-contaminants can be simultaneously removed from water by hybrid GAC sorbents impregnated with iron (hydr)oxide nanoparticles [16–19]. This, in turn, allows for design of small and inexpensive point-of-use water treatment systems capable of removing arsenic and co-contaminants from water sources used by small and rural communities.

In addition to iron (hydr)oxide nanomaterials, many other metal (hydr)oxide nanomaterials have shown promising arsenic removal properties [20]. Some of them, such as zirconium dioxide

* Corresponding author. Tel.: +1 480 727 1291; fax: +1 480 727 1684.
E-mail address: Kiril.Hristovski@asu.edu (K. Hristovski).

0304-3894/$ – see front matter © 2011 Elsevier B.V. All rights reserved.
doi:10.1016/j.jhazmat.2011.07.061

Table 1
Surface area and zirconium content of granulated activated carbon media types used in the study.

Media type	BET surface area (m^2/g)	Zirconium content (%Zr)
Untreated bituminous GAC media	847 ± 12	NA
Bituminous Zr–GAC media	903 ± 4	9.5
Untreated lignite GAC media	696 ± 5	NA
Lignite Zr–GAC media	615 ± 2	12

nanoparticles, can be used to create hybrid metal (hydr)oxide GAC media capable of simultaneously removing arsenic and organic co-contaminants. Zirconium dioxide nanoparticles can be synthesized inside the pores of GAC media using in situ techniques similar to those used in fabrication of hybrid iron (hydr)oxide GAC media. The synthesis process changes the properties of the media, which may affect the arsenic and organic co-contaminant removal abilities of the media. However, although only a handful of attempts have been made to fabricate hybrid zirconium dioxide GAC media for arsenic removal, almost nothing is known about impact of the in situ ZrO_2 nanoparticle formation on the properties of the sorbent GAC media and the consequent arsenic and organic co-contaminant removal [13].

The goal of this study was to investigate the effect of in situ ZrO_2 nanoparticle formation on properties of granulated activated carbon and the consequent impact on arsenic and organic co-contaminant removal performance of the media. To better understand this relationship between the change in media properties and contaminant removal performance, the following objectives were formulated and achieved: (1) novel hybrid zirconium dioxide nanoparticle modified GAC (Zr–GAC) media using two different types of GAC base media were synthesized; (2) the properties of both the new hybrid media and the untreated media were characterized and compared; (3) adsorption capacities of these media for arsenic under equilibrium conditions were estimated; (4) impact of zirconium impregnation on the GAC's organic adsorption capacity was evaluated; and (5) the effects of competing ions on arsenic adsorption under equilibrium and continuous flow conditions was assessed.

2. Experimental approach

Considering that a number of commercially available GAC media with different physico-chemical properties exist, this study had to be limited to only two types of GAC media with distinctively different physical properties. For this study, a bituminous GAC medium and a lignite GAC medium were used as base materials to synthesize hybrid Zr–GAC media. Both untreated GAC media are commercially produced by Norit Americas Inc. (Marshall, TX, USA) and are available in 12 × 40 U.S. mesh size. The lignite based GAC is produced from geologically younger coal material and is not exposed to the same reducing conditions as the coal used to produce bituminous GAC [21]. As a result, the lignite based GAC contains more impurities such as silica, sulfur, and other contaminants, and it exhibits a macroporous structure [14].

2.1. Media synthesis

Table 1 summarizes types and properties of the untreated GAC (V-GAC) used to synthesize Zr–GAC media. ZrO_2 nanoparticles were synthesized inside the pores of the GAC media through a modification of a synthesis method described by Hristovski et al. [22]. In brief, 50 mL of GAC were gently mixed with 100 mL of 2.7 M solution of $ZrOCl_2{\cdot}8H_2O$ precursor for a period of 6 h in a rotating mixer at 30 rpm. The excess zirconium salt solution was then decanted and gently mixed with 5% NaOH for a period of 30 min to precipitate $ZrO(OH)_2$ inside the pores of the GAC material. The excess hydroxide was removed from the zirconium treated media by repeated rinsing with ultrapure water until the decanted solution exhibited pH < 8. The zirconium treated media was then air-dried in negative pressure environment at room temperature. The air-dried media was heated in an inert gas environment at 400 °C for a period of 12 h to anneal the $ZrO(OH)_2$ and convert it to ZrO_2. Ultrapure argon mixed with 5% of hydrogen was used as inert gas to eliminate potential oxidation and minimize any surface changes within the GAC material. The synthesized Zr–GAC media were then soaked in ultrapure water and stored wet before use.

2.2. Media characterization and analytical methods

Zirconium contents of the Zr–GAC media were determined by digestion in a mixture of concentrated HNO_3 and HF acids (US EPA SW-846, Method 3052) followed by inductively coupled plasma optical emission spectroscopy (ICP-OES) analysis for zirconium (Themo iCAP6300 by Thermo Fisher Scientific). Before the acid digestion, samples were ground to a powder and dried at 104 °C to constant mass to remove any moisture. Arsenic concentration was analyzed using a graphite furnace atomic absorption spectrophotometer (GF-AAS) (Varian Zeeman Spectra 400). Methylene blue concentration was measured using UV/vis spectrophotometer (Jenway 6405, Barlow Scientific, Ltd.) at its peak wavelength of 668 nm [23].

Focus ion beam and scanning electron microscopy (FIB/SEM) techniques were used to determine the size and shape of the deposited ZrO_2 nanoparticles within the pores of the media (Nova 200 NanoLab UHR FEG by FEI). A backscatter detector operated in high-resolution immersion mode was used to differentiate between heavier elements such as zirconium, which appear as white areas, and lighter elements such as carbon, oxygen and hydrogen, which appear as darker areas. Energy dispersive X-ray microanalysis (EDX) was used for assessing the elemental distribution of zirconium inside the GAC media.

The surface charges and iso-electric points of the media were estimated by measuring the zeta potential (ZetaPALS by Brookhaven Instrument Corporation) at different pH values in 10 mM KNO_3 background electrolyte solution. The pH was adjusted by drop-wise addition of KOH and HNO_3. X-ray diffraction (XRD) of the finely powdered samples of the synthesized media was analyzed using high resolution X-ray difractometer (PANalytical, X'Pert Pro, CuKα source). The obtained spectra were compared to an existing library of spectra to identify the crystalline structure of ZrO_2. The density and porosity of all media in bulk were estimated following a procedure described in Sontheimer et al. [14]. Surface areas of the samples were determined using the Brunauer–Emmet–Teller (BET) method, while the pore size distributions were determined using the BJH model (MicroMeritics Tristar-II 3020 automated gas adsorption analyzer).

2.3. Multi-point batch equilibrium adsorption tests

The arsenic adsorption capacity of the media was evaluated in batch adsorption tests at pH 7.6 ± 0.2, which is representative of naturally occurring waters. Two model waters were used in these experiments: (1) model 5 mM $NaHCO_3$ buffered ultrapure water with initial arsenic concentration of $C_0 \approx 120$ μg/L and no competing ions was used to assess the maximum adsorption capacity of the media; and (2) model groundwater with same initial arsenic concentration but with competing ions to assess the arsenic adsorption capacity under realistic conditions. The model groundwater containing contaminants that compete with arsenic was characterized as described in Table 2. It was similar to NSF 53 Challenge water

Table 2
Properties of model groundwater matrix containing contaminants competing with arsenate.

Contaminant species	Concentration of ion (mg/L)
N (as NO_3^-)	1.60
F^-	1.10
PO_4^{3-}	0.069
B^-	6.60
Pb(II)	0.002
Cr(III)	0.001
Fe(III)	0.075
Mn(II)	0.029
V(III)	0.007
Se(IV)	0.003
As(V)	0.12
Al(III)	0.046
Cu(II)	0.031
Zn(II)	0.101
Mo(VI)	0.007
SiO_2	20
Mg^{2+}	12
SO_4^{2-}	197
Ca^{2+}	40

[24]. Teflon lined amber glass 250 mL bottles were used as reactors. Media dosages ranged from 0.03 to 0.65 g dry media L^{-1}.

To examine the effect of the ZrO_2 nanoparticle formation on the organic contaminant adsorption capacity of the Zr–GAC media, batch adsorption tests with methylene blue were conducted in 1 mM $NaHCO_3$ ultrapure water at pH 7.5 ± 0.2. Methylene blue has been used in many published studies as a model organic contaminant for organic dyes and natural organic matter [25]. The initial concentration of methylene blue was 50 mg/L. The limitations imposed by the analytical tools used and the high adsorption capacity of GAC for this organic contaminant mandated use of such high initial concentrations.

Adsorption of both arsenate and methylene blue were modeled using the Freundlich isotherm model [14]:(1)$q_e = K_A C_E^{1/n}$where q_e = adsorption capacity (mg adsorbate/g adsorbent); K_A = Freundlich adsorption capacity parameter (mg adsorbate/g adsorbent)(L/mg adsorbate)$^{1/n}$; C_E = equilibrium concentration of the contaminant in solution (mg adsorbate/L); and $1/n$ = Freundlich adsorption intensity parameter (unitless).

2.4. Short bed adsorber column test

Short bed adsorber (SBA) column tests were conducted on both the bituminous and lignite based Zr–GAC to assess the effects that competing ions have on adsorption capacity of the adsorbent for arsenic under continuous flow conditions. Approximately 3.8 mL of media (bed depth ≈ 4.0 ± 0.1 cm) was packed atop a support of quartz sand in a glass column with diameter 1.1 cm. Glass beads were placed above and below the media to provide evenly distributed flow. The mass of the media was ∼1.9 ± 0.1 g. In the tests, the ratio of the column diameter to geometric mean particle diameter was >13. According to Knappe et al. [26], particle diameter to inside column diameter ratios >8 are sufficiently large to neglect the wall-effect on contaminant mass transfer for GAC media which have irregular particle shape. The SBA columns were operated at hydraulic loading rates of 2.8 L/m^2/s (∼4 GPM/ft^2), which are commonly applied to commercial GAC packed bed adsorbers [27]. The empty bed contact time (EBCT) was very short (EBCT ∼14.3 s). The influent arsenic concentration was ∼120 μg/L. Since a minimum of 30 mL of sample volume was needed to conduct the necessary analyses, effluent from the SBA test was collected in ∼20 bed volume (BV) sample aliquots. The column test arsenic adsorption capacity was estimated by calculating the area above the breakthrough curve as described with Eq. (2):

$$\int_0^{m_t} dm_{As} = Q \times \int_0^t C_{ADS}(t)dt \quad (2)$$

where m_{As} is the mass of adsorbed arsenic onto the hybrid media ([M]); Q is the flowrate in the packed bed ([L]^3[T]); $C_{ADS}(t)$ is the difference between the initial and effluent arsenic concentrations at time t ([M][L]$^{-3}$).

To obtain the continuous flow adsorption capacity, the obtained mass for adsorbed arsenic was divided by product of the dry mass of the media used in the packed bed and the zirconium content fraction (Eq. (3)):

$$q_{As} = \frac{m_{As}}{m_{Dry\ media} \times f_{Zr}} \quad (3)$$

where $m_{Dry\ media}$ is the mass of the dry hybrid adsorbent media used in the packed bed column (g dry media); f_{Zr} is the zirconium content fraction; and q_{As} is the adsorption capacity of the dry media (mg As/g Zr).

3. Results and discussion

3.1. Media characterization

Prior to Zr–GAC synthesis, both types of untreated GAC media (lignite and bituminous) exhibited no zirconium content (Table 1). After the synthesis, the zirconium content of the lignite based Zr–GAC increased to a per dry media (∼16.2% of ZrO_2). The zirconium content of the bituminous Zr–GAC was ∼9.5% Zr per dry media (∼12.8 ZrO_2), which was about 20% lower than its lignite based counterpart. This finding is important because it implies that the type of GAC used as a base material has an impact on the overall zirconium content of the final synthesized media since both media were synthesized using the same in situ synthesis method and under the same conditions.

In addition to its effect on zirconium content, the type of GAC media appeared to have an effect on the morphology of the zirconium nanoparticles in the Zr–GAC media. The FIB/SEM microscopy revealed that in situ precipitation of the ZrO_2 resulted in nanostructures with different morphology. Fig. 1a illustrates the presence of patches comprised of berry-like ZrO_2 nanoparticles with sizes ranging from ∼10 to ∼40 nm that formed inside the pores of the bituminous Zr–GAC media. In contrast, Fig. 1b illustrates the presence of a more uniform coating with a thickness in the nano-range that formed inside the pores of the lignite Zr–GAC. Interestingly, however, sections of this nano thick coating exhibited teeth like structures (arrow in Fig. 1b). This morphological diversity of ZrO_2 nanoparticle structures could be a direct result of a more oxidized surface and macroporous structure of the lignite GAC. Being produced from geologically younger coal, which resides closer to the surface, lignite GAC has more oxygen-containing functional groups (e.g., carboxyl groups) on the surface of its pores. These functional groups exhibit negative charges in neutral or slightly acidic pH environments providing for lower isoelectric points. It can be hypothesized that the positively charged Zr precursor ions (ZrO^{2+}) are attracted by these negative surface charges which results in even distribution of the zirconium precursor material on the surface. Furthermore, the macroporous structure of the lignite GAC is less limiting to the pore transport mechanism that conveys these precursor ions from the bulk solution into the pores of the GAC media. This plausible scenario is supported by the data obtained from both zeta-potential and pore size distribution measurements. The estimated isoelectric point for the untreated lignite GAC was about 0.8 pH units lower than the one of the untreated bituminous

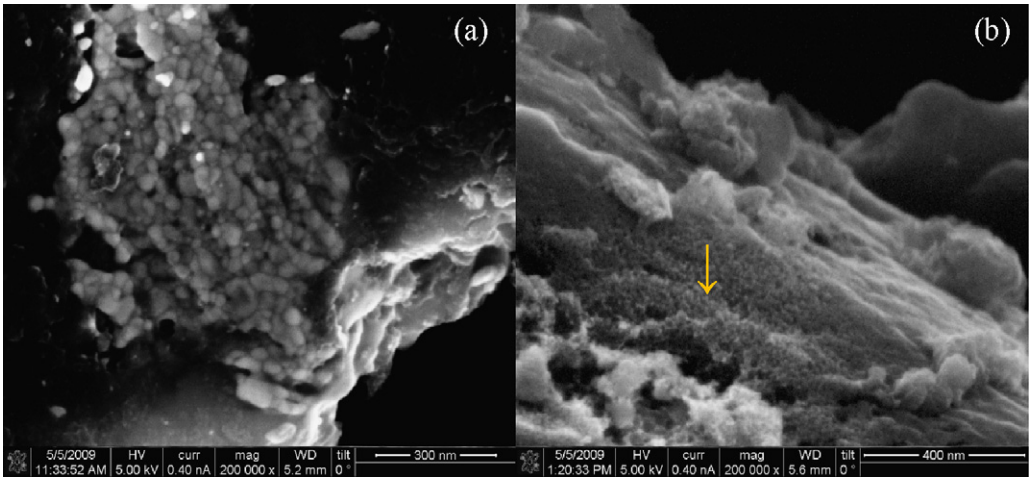

Fig. 1. High magnification FIB/SEM images (200,000×) illustrate the presence of nanoscale ZrO_2 in bituminous (a) and lignite (b) Zr–GAC media. The arrow points at nano-thick coating exhibiting "teeth-like" structures.

GAC (Fig. S1) Additionally, the lignite GAC exhibits a mesoporous and macroporous structure (Fig. 2). This porosity structure of the lignite Zr–GAC allowed for less hindered transport of the relatively large ZrO^{2+} ions, having an unhydrated diameter of ~5 Å [28], into mesopore and low macropore range. In contrast, the data in Fig. 2 shows very little change in the mesopore range of the bituminous Zr–GAC, suggesting that most of the ZrO^{2+} ions did not populate these pores; and instead, majority of the nanoparticles were formed in the macropore region of the bituminous Zr–GAC. The data from the EDX elemental mapping supports the theory that porosity structure has an effect on the transport of ZrO^{2+} ions inside the GAC media (Fig. 3). Zirconium was more evenly distributed throughout the lignite GAC particles than throughout bituminous GAC particles, which exhibited higher zirconium deposition in the outer layers.

Table 1 also summarizes the surface area results for the GAC samples before and after synthesis. Interestingly, the bituminous Zr–GAC exhibited a ~6% increase in surface area after synthesis, while the lignite Zr–GAC exhibited a ~15% loss. The increase in surface area of the bituminous Zr–GAC correlates well with the evidence showing slight increase in the available macropores in the region from ~150 to ~200 nm (Fig. 2) and the type berry-like of nanoparticles (Fig. 1). Formation of berry-like nanoparticles in the macropore region, which has small contribution to the overall surface area, and their negligible formation in the meso and micropore regions, which have large contribution to the overall surface area, could have contributed to the small increase in surface area. In contrast, significant decrease in the lignite GAC mesopore volume was observed after synthesis, which suggests possible pore clogging and blockage of some available mesopores and micropores, consequently resulting in reduced overall surface area. This decrease in mesopore volume correlates well with the FIB/SEM findings for lignite Zr–GAC showing the uniform ZrO_2 coating.

The formation of zirconium dioxide nanoparticle structures resulted in an increase of the isoelectric point for both Zr–GAC media by ~3 pH units relative to the corresponding untreated GAC media (Fig. S1). This is expected as ZrO_2 materials have estimated isoelectric points in the range of ~6.1 to ~6.5 [20]. The XRD spectra (Fig. S2) confirmed the presence of only tetragonal ZrO_2 crystalline structure in both Zr–GAC data implying that the type of GAC base material does not have an impact on the ZrO_2 crystalline structure. Silica, which is commonly found in the form of impurities in coal derived GAC media, was also found to be present in the GAC material. The silica peaks were not visible in the XRD spectra for Zr–GAC media probably because of weak peak intensity when compared to the ZrO_2 peaks. Presence of silica in the GAC media can impact the surface charge of the media because it has very low pH_{IEP} of about 2.0. Considering that lignite GAC usually exhibits higher silica content than its bituminous counterpart, the lower isoelectric points of the lignite GAC and Zr–GAC media are expected [29,30]. An increase in isoelectric point is favorable for media expected to remove negatively charged oxo-ions, such as arsenate and phosphate, in natural waters.

3.2. Effect of zirconium dioxide nanoparticle formation on arsenic adsorption properties

The arsenic equilibrium adsorption data fitted with the Freundlich isotherm model are presented in Fig. 4 for both types of Zr–GAC media and both types of model water. The adsorption capacities of the Zr–GAC media are expressed per mass of zirconium so that it can be easily compared with the adsorption capacities of other metal-containing adsorbents. The bituminous Zr–GAC exhibited slightly higher adsorption capacity than its lignite based Zr–GAC counterpart for both model water matrices. These findings correlate well with the higher surface area of the bituminous Zr–GAC, the formation of new pores and the higher iso-electric point. Interestingly, however, this media had lower zirconium content than the lignite based counterpart, which suggests that most of the ZrO_2 in the lignite Zr–GAC was not accessible either because of pore blockage or because of formation of larger particles (or thicker ZrO_2 layers). Both the pore size distribution and the FIB/SEM data

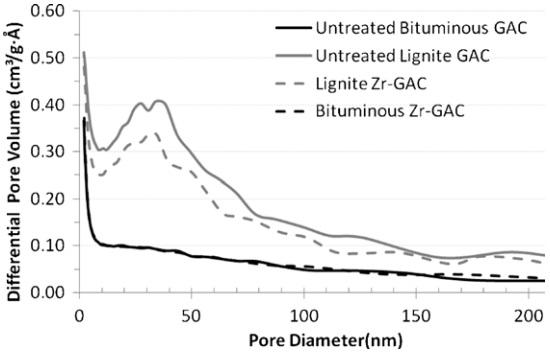

Fig. 2. Differential pore volume as a function of pore diameter for untreated and Zr–GAC media.

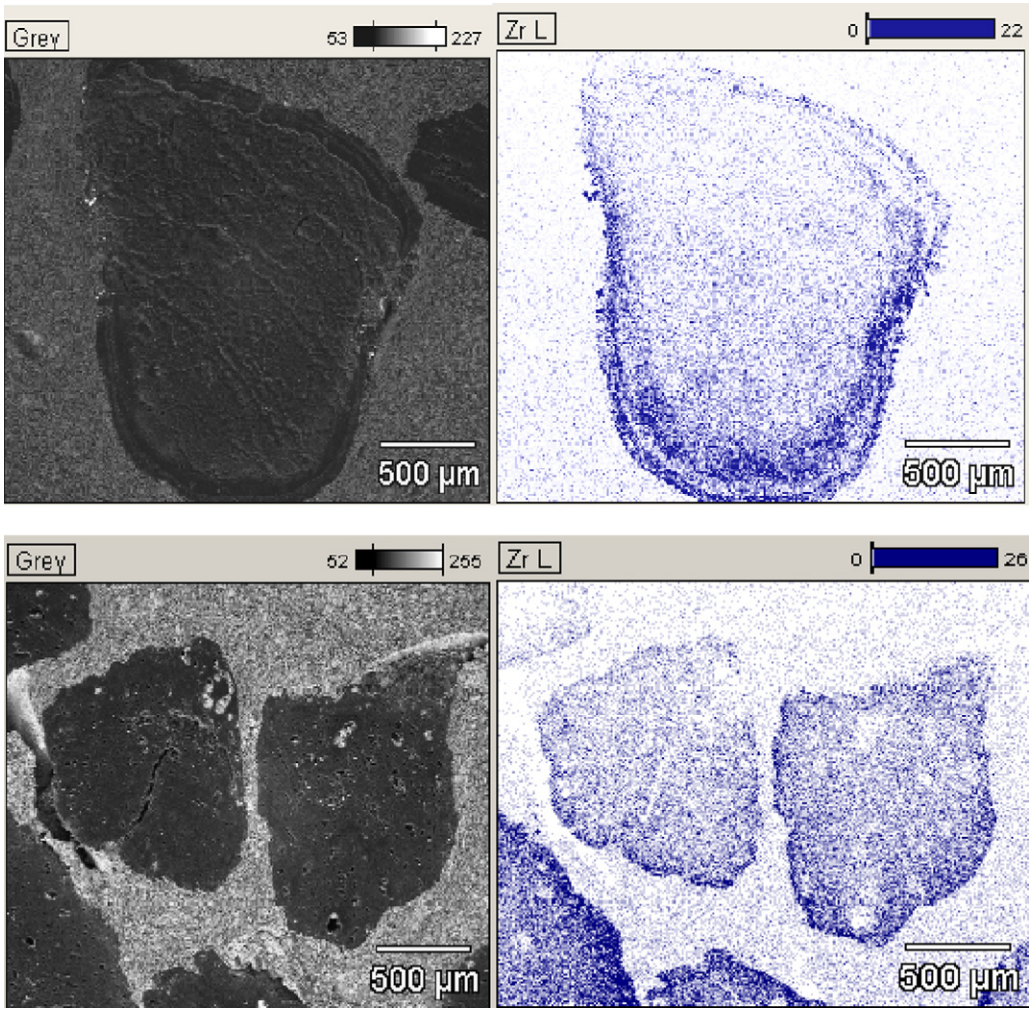

Fig. 3. Elemental distribution of zirconium in bituminous (top) and lignite (bottom) Zr–GAC media.

(Fig. 1) support this hypothesis. In contrast to the Zr–GAC media, the untreated GAC media did not exhibit arsenic removal.

The arsenic Freundlich adsorption intensity parameters ($1/n$) for both Zr–GAC media in both model waters were generally $\leq$0.66 (Fig. 4). Values for $1/n < 1$ generally suggest favorable adsorption. This is not surprising for model water where there is no competing ions, such as phosphate, silica and other oxo-anions, that form inner-sphere bidentate and monodentate ligands with metal

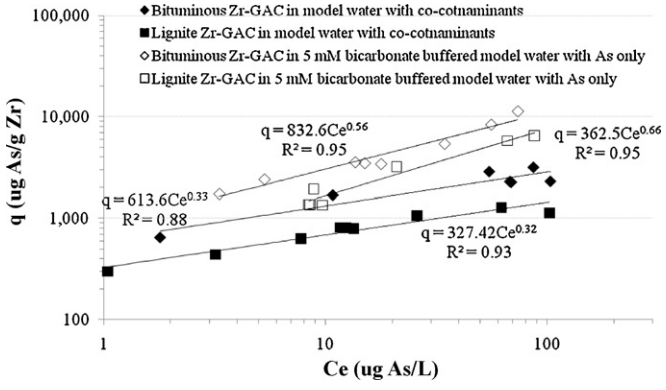

Fig. 4. Freundlich equilibrium adsorption isotherms for arsenic removal by Zr–GAC media in two model waters (pH 7.6 ± 0.2; contact time 3 days; $C_{As\text{-}Initial} \approx 120$ µg/L).

(hydr)oxides. In the presence of competing ions, the $1/n$ value usually tends to increase because competing ions take many of the available sites for arsenic to adsorb by forming bidentate ligands, contributing to the most thermodynamically stable state (lowest adsorption energy) [12,31]. However, this was not the case with both Zr–GAC media. The Freundlich adsorption intensity parameters in matrices with competing ions decreased for both media to $1/n \leq 0.33$. This finding suggests that the presence of competing ions, which increased the ionic strength of the water matrix, lowered the adsorption energy for arsenic. For well hydrated surfaces, the magnitude of the zeta potential decreases with increase in ionic strength [31]. In this case, the increase in ionic strength could have lowered the electrostatic repulsion between the arsenate oxo-anions and the negatively charged surfaces, consequently leading to lower energy of adsorption, i.e., lower $1/n$ values.

The maximum adsorption capacities under the given equilibrium conditions without the presence of competing ions ($q_{0\text{-BICARB}}$) were much higher than the values reported for nano-zirconium oxide media [20,22] assessed under the same conditions (Table 3). The lignite Zr–GAC media removed ~8.6 mg As/g Zr, while bituminous Zr–GAC removed ~12.2 mg As/g Zr when no competitive oxo-anions were present. Commercially available ZrO_2 nanopowders and synthesized ZrO_2 nanostructured spheres removed ~3.5 mg/g Zr and ~2.4 mg/g, respectively, when evaluated in bicarbonate buffered water matrices with no competing oxo-anions. This finding suggests that approaches where ZrO_2 nanoparticles

Table 3
Comparison of maximum arsenic adsorption capacity values for both Zr–GAC media and published values for other metal (hydr)oxide based media evaluated under comparable conditions.

Media type	$q_{0\text{-BICARB}}$ (mg As/g Zr or Fe)	$q_{0\text{-GW}}$ (mg As/g Zr or Fe)	$q_{0\text{-SBA}}$ (mg As/g Zr or Fe)
Zr–GAC (lignite)	~8.59	~1.52	~0.42
Zr–GAC (bituminous)	~12.21	~2.99	~0.89
ZrO_2 nanopowder [20]	~3.51	NA	NA
ZrO_2 nanostructure spheres [22]	~2.35	NA	NA
Granulated ferric hydroxide* [44]	NA	~3.13	NA
Granulated* ferric hydroxide [45]	NA	~2.5	NA
Fe–GAC (pH 6.4) [19]	~6.39	NA	NA
Fe–GAC (pH 8.3) [19]	~1.63	NA	NA

* Considered ~60% Fe content in GFH, pH 7 and C_{eq} = 100 μg/L.

are deposited onto high surface area materials could produce better performing media for arsenic treatment than approaches that focus on aggregated of ZrO_2 nanoparticles.

The maximum equilibrium arsenic adsorption capacities under the given equilibrium conditions decreased by several fold when the water matrices were switched from 5 mM $NaHCO_3$ to model groundwater with competing oxo-anions (Table 3). In the presence of competing oxo-anions, the lignite Zr–GAC removed ~1.5 mg As/g Zr, while bituminous Zr–GAC removed ~3.0 mg As/g of Zr. Silica, phosphate, vanadate, and other oxo-anions in the model water compete with arsenic for the available adsorption sites on metal (hydr)oxides [32–37]. This decrease in adsorption capacity can be primarily attributed to a high concentration of silica in the model groundwater, which was >150 times greater than the concentration of arsenate and other oxo-anions such as phosphate, selenate and vanadate. Soluble silica species and other oxo-anions exhibit high affinity for surfaces of metal (hydr)oxides (e.g., iron oxides/hydroxides) [38–40]. Interestingly, however, the maximum equilibrium adsorption capacities of the media were relatively high and comparable to removal capacities of iron (hydr)oxides under similar conditions when expressed on a per unit mass of metal basis (Table 3), suggesting that surface area may be the largest contributing factor to high adsorption capacity of zirconium oxide based media, especially if the newly created surface area is in the macropore region.

Fig. 5 illustrates the breakthrough curves used to determine the continuous flow adsorption capacity ($q_{max\text{-}SBA}$) for both Zr–GAC media. Although the breakthrough curves look very similar, the calculations showed that the continuous flow adsorption capacity of the lignite Zr–GAC remained lower (~425 μg As/g Zr) when compared to the bituminous counterpart (~890 μg As/g Zr). This difference could be a result of the higher Zr content of lignite Zr–GAC. Interestingly, however, the capacities of both Zr–GAC media were ~3.5 times lower than their maximum adsorption capacities under equilibrium conditions ($q_{0\text{-GW}}$) in the same model groundwater. This suggests that mass transport has an effect on contaminants' competition for available adsorption sites. Liquid diffusivity, describing a solutes liquid phase movement, is largely dependant on the size and charge of the ion and the temperature of the fluid. Contaminant species with higher D_l values experience lower film and intraparticle resistance and can diffuse much faster inside the pores of the particle than arsenate, which allows them to reach unoccupied adsorption sites much faster than arsenic [14]. This effect is favorable for oxo-anions with higher liquid diffusivities than arsenate, such as silica, phosphate, or selenate ($D_{l\text{-Silica}} \approx 1.170 \times 10^{-5}$ cm^2/s; $D_{l\text{-dihydrogen phosphate}} \approx 0.959 \times 10^{-5}$ cm^2/s; $D_{l\text{-Selenate}} \approx 1.008 \times 10^{-5}$ cm^2/s; $D_{l\text{-Arsenate}} \approx 0.905 \times 10^{-5}$ cm^2/s), [41,42]. Considering that these oxo-anions also form strong inner-sphere complexes, it is very difficult for arsenate to displace them once they adsorb onto the metal (hydr)oxide surfaces. The overall effect could result in a several fold decrease of arsenic adsorption capacity of the media.

3.3. Effect of zirconium dioxide nanoparticle formation on methylene blue adsorption

Fig. 6 shows Freundlich isotherms for methylene blue adsorption onto untreated GAC and Zr–GAC media in both model waters. Interestingly, the methylene blue adsorption capacity of the lignite based media did not change after impregnation with the ZrO_2. The bituminous Zr–GAC exhibited higher adsorption capacity than its lignite counterpart in both model waters. However, this adsorption capacity decreased once the untreated bituminous GAC media was impregnated with ZrO_2. These findings do not seem surprising considering factors such as: (1) the pore size distribution of these media (before and after treatment); (2) the size of hydrated methylene blue molecule, and (3) the calculated Freundlich adsorption intensity parameters. As summarized in Fig. 5, the $1/n$ values for both

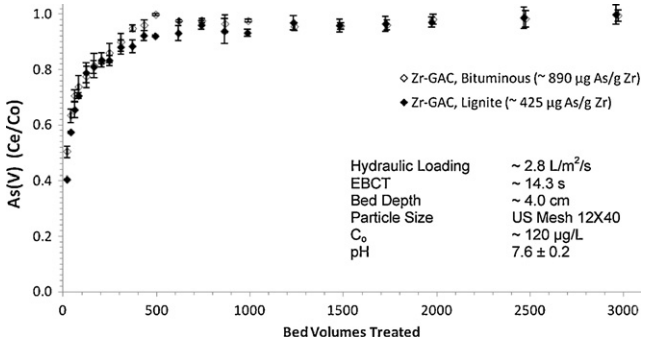

Fig. 5. Breakthrough curves for arsenic in continuous flow short packed bed adsorber tests in model groundwater with competing oxo-anions (error bars represent standard deviations).

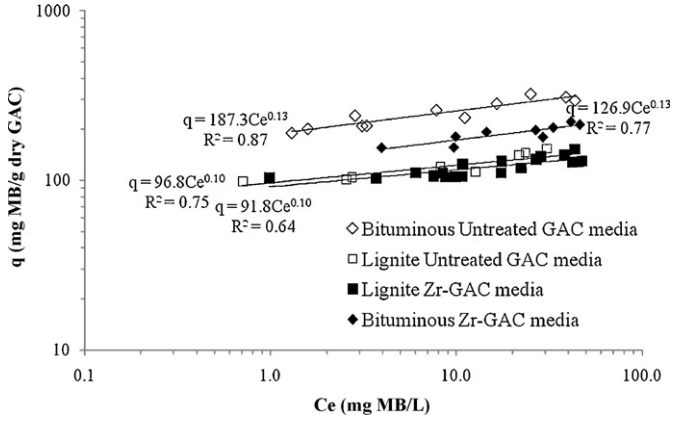

Fig. 6. Freundlich equilibrium adsorption isotherms for methylene blue (MB) removal by untreated and Zr–GAC media in 1 mM $NaHCO_3$ buffered ultrapure water (pH 7.5 ± 0.2; contact time 3 days; $C_{MB\text{-Initial}} \approx 50$ mg/L).

media types did not appreciably change after treatment. This trend suggests that the energies of adsorption remained the same due to absence of significant change in properties of the carbon surfaces, meaning that the change in adoption capacity of the bituminous based media was caused by physical blockage of carbon surfaces in the macropore range, rather than chemical change of carbon surface properties. This concept is further supported by the findings presented in Fig. 2. As discussed above, formation of new pores and surface area in the bituminous Zr–GAC occurred in the region of ~150 nm to 200 nm due to ZrO_2 nanoparticle formation. The ZrO_2 nanoparticle formation resulted in blocking the carbon surfaces in this region available for methylene blue adsorption. The hydrated methlylene blue molecule could not adsorb in the micropore and mesopore region where carbon surface was not changed because of its large size (>7 × 16 Å) [43]. The lignite Zr–GAC media retained its adsorption capacity for methylene blue, even though the surface area decreased. In this case, however, most of the decrease in surface area and pore volume occurred in the micropore and mesopore region. Although the macropore region did exhibit a slight decrease in pore volume, this decrease did not significantly impact the adsorption capacity for methylene blue.

3.4. Economic feasibility

Although hybrid media for multiple contaminant removal may be more expensive than the commercially available metal (hydr)oxide media, the latter ones do not have the ability to remove multiple contaminants with different chemistries. Implementing solutions utilizing treatment trains with multiple media to treat organic and inorganic contaminants may not be economically feasible in small and rural communities because of the high cost of construction, operation and maintenance. Small point-of-use treatment systems packed with hybrid adsorbents may provide cost effective alternatives.

Only a fraction of the metal precursors are used during fabrication of the hybrid materials when compared to the commercially available metal (hydr)oxide sorbents, which can lead to significant cost reduction. The cost manufacturing could be further reduced if cheaper precursor materials are used such as ferric based salts. However, the substitution of zirconium with iron may not be suitable for applications where the pH needs to be decreased in order to increase arsenic adsorption capacity and minimize the effects of competing silica. The stability of the zirconium dioxide over ferric (hydr)oxides under lower pH conditions may prove to be the deciding factor over small cost difference.

4. Conclusions

The findings in this study imply that properties of granular activated carbon have a significant impact on the formation, morphology and distribution of the ZrO_2 nanoparticles. The modification of the bituminous GAC with ZrO_2 nanoparticles resulted in slightly higher surface area and negligible change in the overall micro and mesopore volume probably because the nanoparticles formed in its macroporous region, making them more accessible to potential contaminants. In contrast, the lignite Zr–GAC exhibited decrease in surface area because the nanoparticles formed in the mesoporous and low range macroporous region. The increased surface area and better accessibility to the ZrO_2 nanoparticles could be attributed to the better arsenic removal performance of the bituminous Zr–GAC under equilibrium and continuous flow conditions.

Zirconium metal oxide based hybrid media may offer a viable alternative to other metal (hydr)oxide hybrid based media for simultaneous removal of multiple inorganic (e.g., arsenic) and organic contaminants. It was demonstrated that there was little to no impact on the adsorption capacity of organic contaminates with the Zr–GAC's. As shown in this study, proper selection of GAC media with adequate porosity and suitable surface area and properties may transform GAC media into media with arsenic adsorption capacities comparable to commercially available ferric (hydr)oxides when expressed on basis of metal content. However, the commercially available ferric (hydr)oxides lack the ability to simultaneously remove organic contaminants, which is the main advantage of using hybrid sorbents in water treatment applications such as small point-of-use systems.

Acknowledgments

A large portion of this work was supported by the Southwest Consortium for Environmental Research and Policy (SCERP) though a cooperative agreement with the U.S. Environmental Protection Agency. SCERP can be contacted for further information through www.scerp.org and scarp@mail.sdsu.edu.

Appendix A. Supplementary data

Supplementary data associated with this article can be found, in the online version, at doi:10.1016/j.jhazmat.2011.07.061.

References

[1] R. Nickson, J. McArthur, W. Burgess, K.M. Ahmed, P. Ravenscroft, M. Raman, Arsenic poisoning of Bangladesh groundwater, Nature. 395 (1998), 338–338.
[2] R. Nickson, C. Sengupta, P. Mitra, S.N. Dave, A.K. Banerjee, A. Bhattacharya, S. Basu, N. Kakoti, N.S. Moorthy, M. Wasuja, M. Kumar, D.S. Mishra, A. Ghosh, D.P. Vaish, A.K. Sprivastava, R.M. Tripathi, S.N. Sinsh, R. Prasad, S. Bhattacharya, P. Deverill, Current knowledge on the distribution of arsenic in groundwater in five states of India, J. Environ. Sci. Health Part A 42 (2007) 1707–1718.
[3] J. Matschullat, Arsenic in the geosphere—a review, Sci. Total Environ. 249 (2000) 297–312.
[4] United States, Implementation Guidance for the Arsenic Rule, United States Environmental Protection Agency, Office of Water, Washington, D.C, 2002.
[5] WHO (Ed.), Guidelines for drinking-water quality, 3rd ed., World Health Organization, Geneva, 2004.
[6] EU Council, Council directive 98/83/EC of 3 November 1998 on the quality of water intended for human consumption, Off. J. Eur. Commun. L330 (1998) 32–54.
[7] A. Kovski, EPA recalculation of cancer risk for arsenic could have costly impact on many industries, Environ. Reporter – Bureau Natl. Affairs Inc. 40 (36) (2009) 2138–2139.
[8] US Department of Health and Human Services (Ed.), Toxicological Profile for Arsenic, US Department of Health and Human Services, Washington DC, 2000.
[9] P.L. Smedley, D.G. Kinniburgh, A review of the source, behaviour and distribution of arsenic in natural waters, Appl. Geochem. 17 (2002) 517–568.
[10] F.A. Cotton, G. Wilkinson, Advanced Inorganic Chemistry; A Comprehensive Text, 3rd ed., Interscience Publishers, New York, 1972.
[11] N. Greenwood, A. Earnshaw, Chemistry of the Elements, 2nd ed., Reed Educational and Professional Publishing Ltd, Woburn, MA, USA, 1997.
[12] S.R. Randall, D.M. Sherman, Surface complexation of arsenic(V) to iron(III) (hydr)oxides: structural mechanism from ab initio molecular geometries and EXAFS spectroscopy, Geochim. Cosmochim. Acta 67 (2003) 4223–4230.
[13] D. Mohan, C.U. Pittman Jr., Arsenic removal from water/wastewater using adsorbents—a critical review, J. Hazard. Mater. 142 (2007) 1–53.
[14] H. Sontheimer, J. Crittenden, S. Summers, Activated Carbon for Water Treatment, second ed., DVGW-Forschungsstelle, Engler-Bunte Institut, Universitat Karlsruhe, Karlsruhe, Germany, 1988.
[15] B. Daus, R. Wennrich, H. Weiss, Sorption materials for arsenic removal from water: a comparative study, Water Res. 38 (2004) 2948–2954.
[16] G. Muñiz, V. Fierro, A. Celzard, G. Furdin, G. Gonzalez-Sánchez, M.L. Ballinas, Synthesis, characterization and performance in arsenic removal of iron-doped activated carbons prepared by impregnation with Fe(III) and Fe(II), J. Hazard. Mater. 165 (2009) 893–902.
[17] A.M. Cooper, K.D. Hristovski, T. Möller, P. Westerhoff, P. Sylvester, The effect of carbon type on arsenic and trichloroethylene removal capabilities of iron (hydr)oxide nanoparticle-impregnated granulated activated carbons, J. Hazard. Mater. 183 (2010) 381–388.
[18] V. Fierro, G. Muñiz, G. Gonzalez-Sánchez, M.L. Ballinas, A. Celzard, Arsenic removal by iron-doped activated carbons prepared by ferric chloride forced hydrolysis, J. Hazard. Mater. 168 (2009) 430–437.
[19] K. Hristovski, P. Westerhoff, T. Möller, P. Sylvester, Effect of synthesis conditions on nano-iron (hydr)oxide impregnated granulated activated carbon, Chem. Eng. J. 146 (2009) 237–243.

[20] K. Hristovski, A. Baumgardner, P. Westerhoff, Selecting metal oxide nanomaterials for arsenic removal in fixed bed columns: from nanopowders to aggregated nanoparticle media, J. Hazard. Mater. 147 (2007) 265–274.
[21] B. Buecker, Coal (What your parents never taught you.), Power Eng. 110 (2006), 104–104.
[22] K. Hristovski, P. Westerhoff, J. Crittenden, L. Olson, Arsenate removal by nanostructured ZrO_2 spheres, Environ. Sci. Technol. 42 (2008) 3786.
[23] F. Raposo, M.A. De La Rubia, R. Borja, Methylene blue number as useful indicator to evaluate the adsorptive capacity of granular activated carbon in batch mode: influence of adsorbate/adsorbent mass ratio and particle size, J. Hazard. Mater. 165 (2009) 291–299.
[24] K. Hristovski, P. Westerhoff, T. Möller, P. Sylvester, W. Condit, H. Mash, Simultaneous removal of perchlorate and arsenate by ion-exchange media modified with nanostructured iron (hydr)oxide, J. Hazard. Mater. 152 (2008) 397–406.
[25] Q. Qian, Q. Chen, M. Machida, H. Tatsumoto, K. Mochidzuki, A. Sakoda, Removal of organic contaminants from aqueous solution by cattle manure compost (CMC) derived activated carbons, Appl. Surf. Sci. 255 (2009) 6107–6114.
[26] D.R.U. Knappe, V.L. Snoeyink, P. Roche, M.J. Prados, M. Bourbigot, The effect of preloading on rapid small-scale column test predictions of atrazine removal by GAC adsorbers, Water Res. 31 (1997) 2899–2909.
[27] R.M. Clark, B.W. Lykins, Granulated Activated Carbon: Design Operation and Cost, Lewis Publishers, Inc, Clelsea, Michigan, 1989.
[28] C. Hagfeldt, V. Kessler, I. Persson, Structure of the hydrated, hydrolysed and solvated zirconium(IV) and hafnium(IV) ions in water and aprotic oxygen donor solvents. A crystallographic, EXAFS spectroscopic and large angle X-ray scattering study, Dalton Trans. (2004) 2142–2151.
[29] G.A. Parks, The isoelectric points of solid oxides, solid hydroxides, and aqueous hydroxo complex systems, Chem. Rev. 65 (1965) 177–198.
[30] J.A. Schwarz, C.T. Driscoll, A.K. Bhanot, The zero point of charge of silica—alumina oxide suspensions, J. Colloid Interface Sci. 97 (1984) 55–61.
[31] J.C. Crittenden, R.R. Trussell, D.W. Hand, K.J. Howe, G. Tchobanoglous (Eds.), Water Treatment; Principles and Design, 2nd ed., Wiley & Sons, Inc, Hoboken, New Jersey, USA, 2005.
[32] R.K. Iler, The Chemistry of Silica: Solubility, Polymerization, Colloid and Surface Properties and Biochemistry, Wiley, New York, 1979.
[33] W. Zhang, P. Singh, E. Paling, S. Delides, Arsenic removal from contaminated water by natural iron ores, Miner. Eng. 17 (2004) 517–524.
[34] K. Goh, T. Lim, Geochemistry of inorganic arsenic and selenium in a tropical soil: effect of reaction time, pH, and competitive anions on arsenic and selenium adsorption, Chemosphere 55 (2004) 849–859.
[35] C.A. Impellitteri, Effects of pH and competing anions on the speciation of arsenic in fixed ionic strength solutions by solid phase extraction cartridges, Water Res. 38 (2004) 1207–1214.
[36] S. Goldberg, C.T. Johnston, Mechanisms of arsenic adsorption on amorphous oxides evaluated using macroscopic measurements, vibrational spectroscopy, and surface complexation modeling, J. Colloid Interface Sci. 234 (2001) 204–216.
[37] S. Dixit, J.G. Hering, Comparison of arsenic(V) and arsenic(III) sorption onto iron oxide minerals: Implications for arsenic mobility, Environ. Sci. Technol. 37 (2003) 4182–4189.
[38] C.C. Davis, W.R. Knocke, M. Edwards, Implications of aqueous silica sorption to iron hydroxide: mobilization of iron colloids and interference with sorption of arsenate and humic substances, Environ. Sci. Technol. 35 (2001) 3158–3162.
[39] C.C. Davis, H. Chen, M. Edwards, Modeling silica sorption to iron hydroxide, Environ. Sci. Technol. 36 (2002) 582–587.
[40] M. Badruzzaman, Mass transport scaling and the role of silica on arsenic adsorption onto porous iron oxide (hydroxide) Ph.D. Dissertation, Arizona State University (December, 2005).
[41] L. Rebreanu, J. Vanderborght, L. Chou, The diffusion coefficient of dissolved silica revisited, Mar. Chem. 112 (2008) 230–233.
[42] D. Lide (Ed.), CRC Handbook of Chemistry and Physics, 87th ed., Taylor and Francis Group, Boca Raton, Florida, 2006.
[43] S. Sohrabnezhad, A. Pourahmad, M.A. Sadjadi, New methylene blue incorporated in mordenite zeolite as humidity sensor material, Mater. Lett. 61 (2007) 2311K–2314K.
[44] A. Sperlich, A. Werner, A. Genz, G. Amy, E. Worch, M. Jekel, Breakthrough behavior of granular ferric hydroxide (GFH) fixed-bed adsorption filters: modeling and experimental approaches, Water Res. 39 (2005) 1190–1198.
[45] P. Westerhoff, D. Highfield, M. Badruzzaman, Y. Yoon, Rapid small-scale column tests for arsenate removal in iron oxide packed bed columns, J. Environ. Eng. 131 (2005) 262–271.